JCAMECH

Vol. 46, No. 2, July 2015, pp 177- 190

A mesh generation procedure to simulate bimaterials

Mohammad Reza Vaziri Sereshk[1*] and Mohammad Hassan Esmaeili[2]

1. School of Mechanical Engineering, College of Engineering, University of Tehran, Tehran, Iran,

2. Mechanical Engineering Department, University of Kashan, Kashan, Iran

Received: May 1, 2014; Accepted: September 12, 2014

Abstract

It is difficult to develop an algorithm which is able to generate the appropriate mesh around the interfaces in bimaterials. In this study, a corresponding algorithm is proposed for this class of unified structures made from different materials with arbitrary shapes. The non-uniform mesh is generated adaptively based on advancing front technique available in Abaqus software. Implementing several preliminary analyses, the output of each step prepared data source for the next step of mesh generation. After examining several criteria, the mean elemental stress derivative is selected as a suitable criterion to evaluate the performance of current mesh. The convergence indicates non-isometric final mesh with appropriate and optimum distribution. In general, automatic mesh generators determine the mesh density only based on the geometry of the model; however, the developed algorithm modifies mesh after sensing the stress intensity due to various reasons including loading condition and any change in material and geometry. In addition, the proposed algorithm converges to accurate result fast enough if considering the numbers of remeshing steps. An adaptive mesh generator code can be programmed based on the developed procedure to automatically generate mesh if implementing in Abaqus as a subroutine.

Keywords: *adaptive meshing, bimaterials, mesh generation, stress concentration.*

1. Introduction

Since 1960 that finite element (FE) method was born, several engineering softwares have been provided and presented to the market. User-friendly application of the FE softwares motivates the users to progressively implement this especial tool to solve differential equations governing sophisticated engineering problems. Each FE code, including Abaqus [1] and Ansys [2] uses especial mesh generation algorithms as its own characteristics. In general, in order to access optimum mesh, several models with increasing numbers of elements are examined; the convergence is the main criterion to stop this procedure [3]. As an example, Van Miegroet and Duysinx [4] applied a novel shape optimization approach based on the level set description of the geometry and the extended finite element method (X-FEM). However, they only examined their

* Corresponding author Email: m.vaziri@ut.ac.ir

approach for problems with stress concentration only due to geometry. Performing this optimization approach especially for isometric mesh is very time-consuming. The adaptive meshing has been introduced as a solution. In this approach some pre-solution steps indicates where finer mesh is needed [5, 6, 7, 8]. As the pioneer, Paulino et al. [9] introduces a methodology for self adaptive numerical procedures, which relies on the various components of an integrated, object-oriented, computational environment involving pre- analysis, and post-processing modules. The mesh (re-) generation process is accomplished by means of proposed methods combining quadtree, and Delaunay triangulation techniques. Murthy and Mukhopadhyay [10] developed a fully automatic advancing front type mesh generator for especial application. The refinement methodology depends on the concept of strain energy concentration for completely automatic adaptive analysis of mixed-mode crack problems.

The main focus for some adaptive meshing procedure is on geometry. Zhao et al. [11] argued that the exact description of complex geometric features such as holes, slots, and curved surfaces is crucial to the accuracy of finite element analysis. They presented an algorithm for the adaptive generation of the initial hexahedral element mesh based on the geometric features of the solid model. Liang and Zhang [12] presented a novel octree-based dual contouring (DC) algorithm for adaptive triangular or tetrahedral mesh generation. The main purpose was to maintain angle range for triangle mesh in the desired range. Sun and Zhao [13] presented an adaptive mesh generation algorithm for the thin features with small thickness of the geometric model, to successfully implementing each meshing step, containing the techniques for adaptive refinement, boundary match, topological optimization and local refinement.

Other adaptive meshing procedures are developed in a way to sense any change in material. In order to consider real treatment of material in crack propagation simulation, Alshoaibi and Ariffin [14] developed a finite element (FE) program implementing elastic-plastic property. At each propagation step, the adaptive mesh is automatically refined based on a posteriori *h*-type refinement using norm stress error estimator. Ruiz-Girones et al. [15] propose to combine the size-preserving method with a smoothing technique that takes into account both the element shape and size. The size-preserving technique allows directly generating a quadrilateral mesh that reproduces the size function, while the proposed smoother allows obtaining a high-quality mesh during the maintenance of the element size.

Some researchers specifically studied the problems regarding adaptive meshing performance at interfaces of biomaterials. Rajagopal and Sivakumar [16] proposed an adaptive strategy which involves a combination of the configurational force based *r*-adaption with weighted laplacian smoothing and mesh enrichment by *h*-refinement. The study confirms that the proposed combined *r*-*h* adaption is more efficient than a purely *h*-adaptive approach and more flexible than a purely *r*-adaptive approach with better convergence characteristics and helps in obtaining optimal finite element meshes for a specified accuracy. Carson et al. [17] studied the biomechanical problems including the fluid and solid phases share a common interface geometrically. They argued that spatial discretization of complex imaging derived fluid–solid geometries, such as the cardiac environment, is a critical but often overlooked challenge in biomechanical computations. This application opens a new window for the future of this field. More recently Li et al. [18] evaluated interface cracks in piezoelectric bimaterials by extending the scaled boundary finite element method (SBFEM). In this method, a piezoelectric plate is divided into polygons. Each polygon is treated as a scaled boundary finite element subdomain. Only the boundaries of the subdomains need to be discretized by line elements. The benefit of this approach is that no asymptotic solution, local mesh refinement or other special treatments around a crack tip are required.

In this study in order to generate mesh for bimaterials adaptively, an algorithm is developed to sense different reasons of locally rapid changes. The small enough elements are generated in the corresponding region. In order to evaluate the performance of the procedure, different sources of stress concentration are investigated individually and simultaneously in some benchmark problems.

2. The algorithm for mesh generation

The procedure of mesh refinement starts with coarse uniform mesh. After conducting one step of solution, the result is evaluated by identified criterion and the decision is made regarding the size and distribution of the elements for the next step. This procedure is continued to reach the convergence, where the outcome of the analysis does not change in further refinement steps. Figure 1 indicates the steps for developed algorithm.

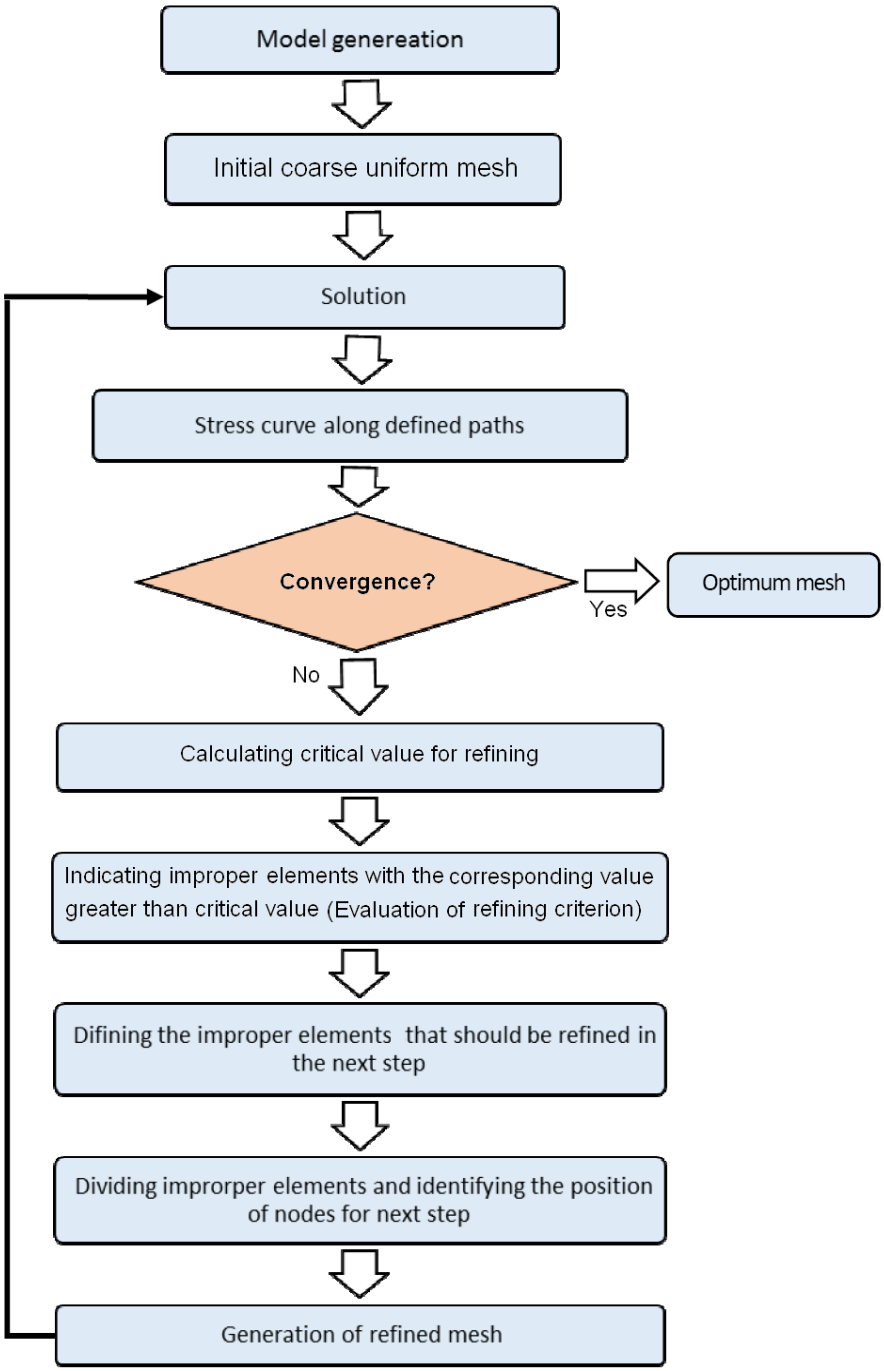

Fig. 1. Developed adaptive mesh generation algorithm

3. The criteria for mesh refinement

To find a suitable criterion, a well-known benchmark problem having closed form solution is investigated [19]. A rectangular plate $1\times 0.5\times 0.01 m^3$ with a $15\ cm$ diameter circular hole is considered subjected to uniformly distributed $10\ kN/m$ load on parallel lateral sides. The $E=207\ GPa$ and $\nu=0.3$ are considered as property for material. The Abaqus software is used to build plane stress 2D model. Figure 2a shows the geometry and loading condition of the whole model partitioned to four similar sections; while Figures 2b and 2c demonstrate initial coarse mesh generated for one quarter of the whole symmetric model and the selected paths around the model, respectively. The paths are selected in a way to be able to implement advancing front mesh generation technique available in Abaqus software. In this technique, the user controls the meshing procedure via selecting proper number and distribution of nodes along each path. As boundary condition, the nodes in paths 1 and 4 are prevented to move in horizontal and vertical directions, respectively.

After each solution step, the stress values are extracted from the output file for the nodes along the paths shown in Figure 2c. Each refinement criterion introduces its own special principal parameter that should not be greater than the identified value. Several criteria are evaluated including deviation from shape function, the average of the maximum and minimum of the derivatives of stress, the average of all nodal stress derivatives, and the average of stress variation along each element. However, dividing element based on these criteria leads to unexpected finer mesh in improper regions, as well as very slow convergence or even divergence. In some cases, the mesh changes significantly after each refinement step. Figure 3 demonstrates the generated mesh after identified refining steps.

3.1. Appropriate stress intensity criterion

It is expected that the mesh in the stress concentration zone should be finer; therefore, the criteria based on the stress derivative is examined as, representative of intensity of stress variation. The definition provided by finite difference method [20] is used to calculate elemental derivative. It is basically the slope of the straight line connecting the nodal stress values for two neighboring nodes in stress variation curve along the path. After examining several limitations, the mean elemental stress derivatives are identified as suitable limit for refinement criterion. Each element with elemental stress derivative greater than this limit is divided into two elements in the mesh refined for the next step of algorithm (Fig. 1).

Considering the initial coarse mesh, the local intensity of stress located near one side of the element may be vanished; therefore, in each refinement step, one element closed to the improper element is also divided into two elements.

In order to investigate the convergence, a suitable path among the paths shows in Figure 2c is selected; if the curve representing variation of the stress along mentioned path does not change considerably after refining process, the process is converged to the optimum mesh and the refining procedure is ended. Figure 4 shows the trend of convergence along the path 5 (Fig. 2c).

It can be seen that the solution converges after only 5 refining steps. The authors also investigated the convergence in other paths. Figure 5 shows generated mesh after the noted number of the refining process.

It is demonstrated in Figures 4 and 5 that the solution converges properly. Since the mesh is sufficiently fine in the stress concentrated zone, the fine and coarse regions of optimum mesh are distributed properly. Figure 6 shows the optimum mesh for the whole model.

3.2. Evaluation of the generated mesh

Two different sources are used to evaluate the performance of described algorithm. One is the result obtained for the mesh generated by adaptive mesh option available in Abaqus; the other one is the exact analytical solution available in some elasticity reference book for this benchmark problem [19]. Using the default setting for adaptive meshing option is available in Abaqus, the convergence is reached after 6 steps; while only 5 refining steps are needed using the developed algorithm. However, there are more elements in optimum mesh corresponding to algorithm. Figure 7 compares the proposed mesh by algorithm and Abaqus.

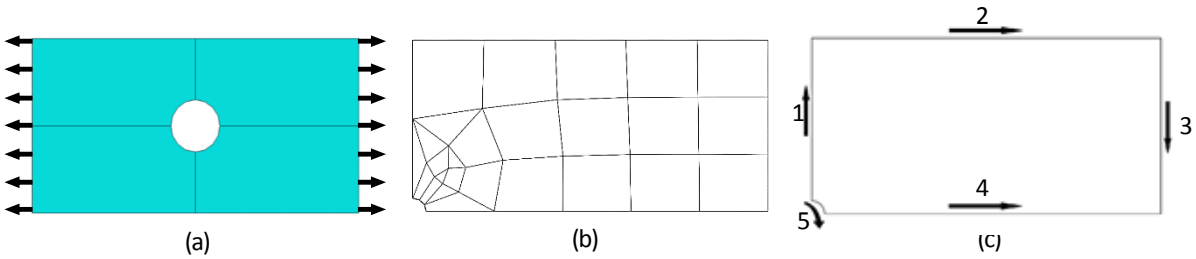

Fig. 2. (a) The geometry and loading condition; (b) mesh generated for a partition; (c) paths around the model

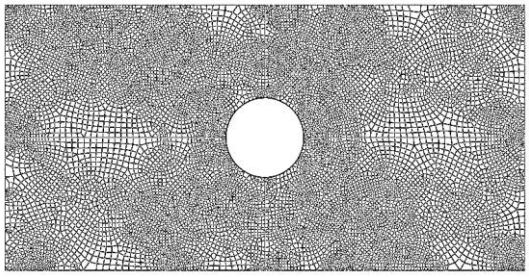

(a) After 25 refining steps with deviation from shape function criterion

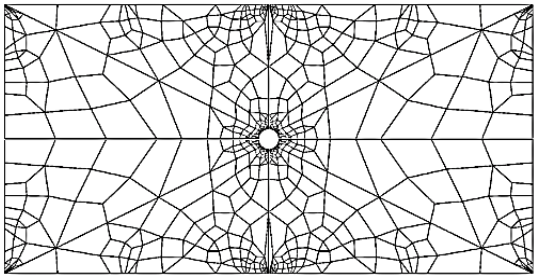

(b) After 10 refining steps with average of maximum and minimum of the derivatives of stress criterion

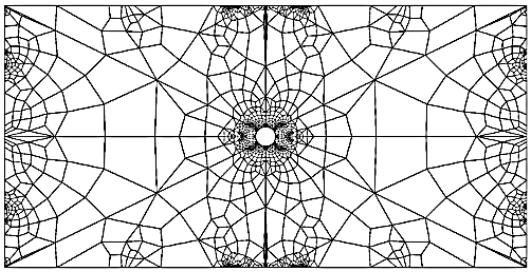

(c) After 10 refining with average of all nodal stress derivative criterion

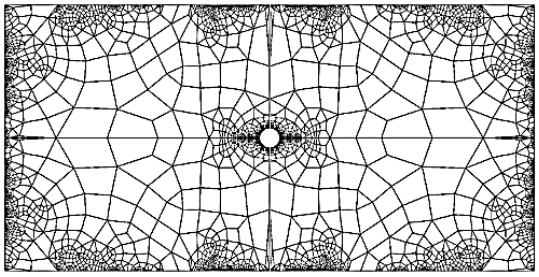

(d) After 10 refining with the criterion as average of stress variations along each element

Fig. 3. Proposed mesh

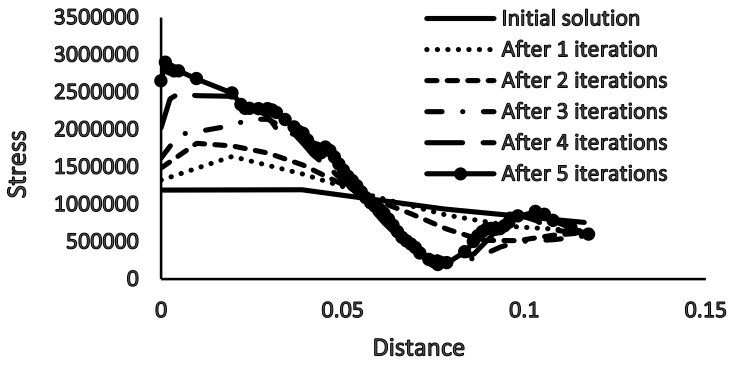

Fig. 4. Convergence of mesh refining process along the path 5

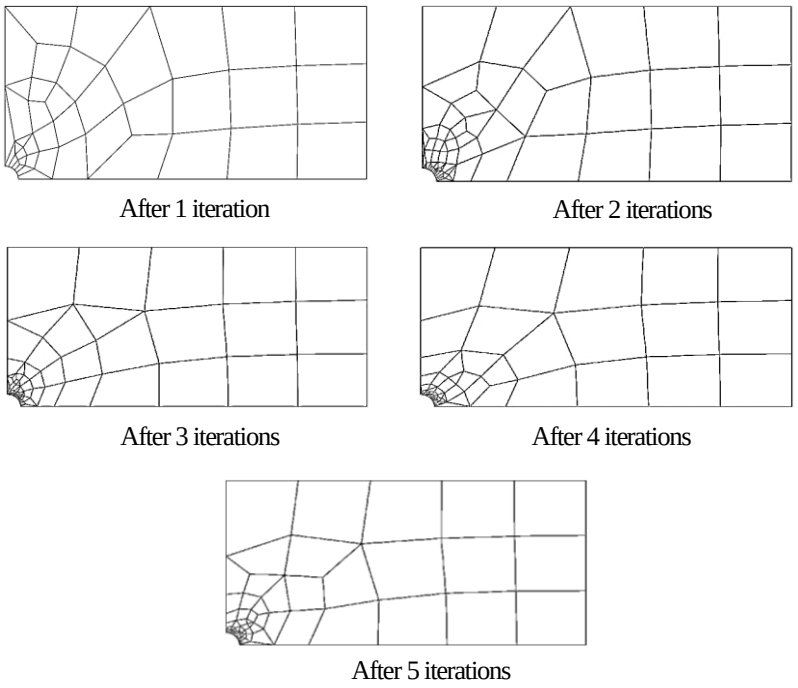

Fig. 5. Generated meshes after the identified number of the refining process

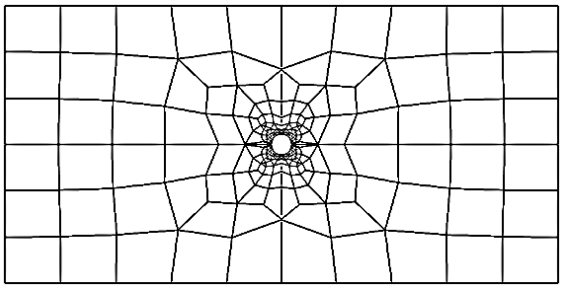

Fig. 6. Optimum mesh obtained by presented algorithm

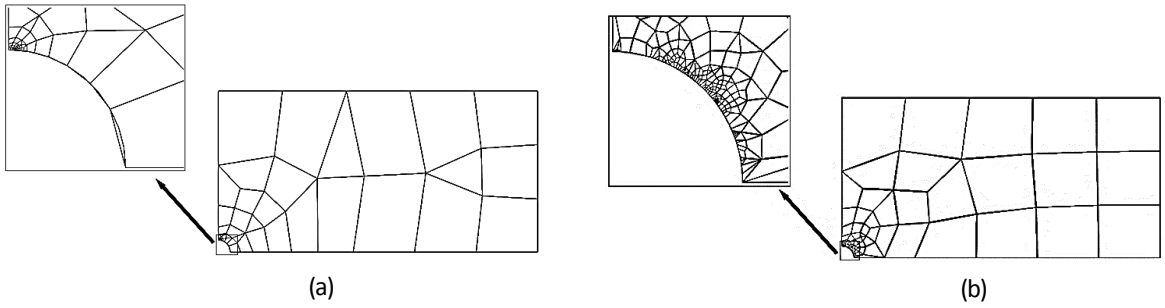

Fig. 7. Mesh proposed by: (a) Abaqus; (b) algorithm

Although the general pattern of meshes is similar in Figure 7, the detailed look reveals the slightly different distribution. To investigat the accuracy, the predicted stress is compared along the paths 1 and 5 (Fig. 2c) in Figures 8 and 9 with the exact solution [19].

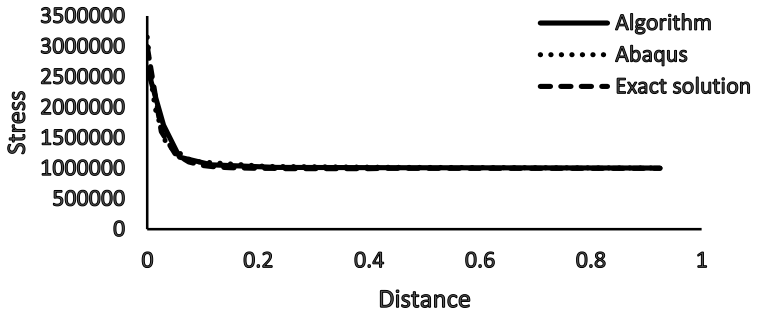

Fig. 8. Predicted stress along path 1

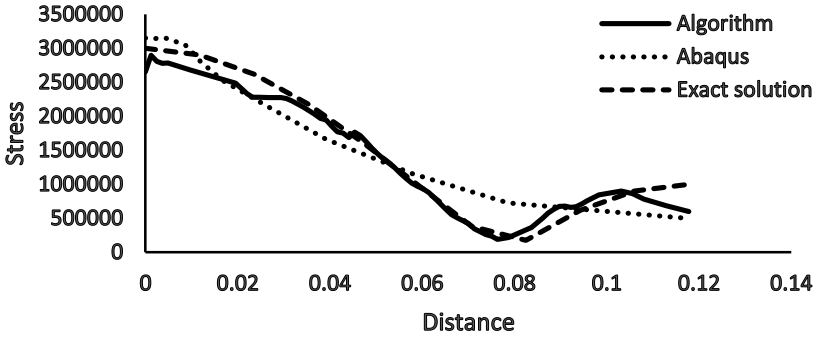

Fig. 9. Predicted stress along path 5

As it can be seen in Figures 8 and 9, good agreement is seen between the results of all three approaches. Therefore, the developed algorithm converges fast enough and presents high quality mesh. Considering that path 5 goes through the stress concentration region, the Figure 5 demonstrates the proper performance of developed algorithm in capturing the stress intensity compared to the available adaptive meshing of Abaqus.

4. Practical application of algorithm

To investigate more general cases, the performance of developed algorithm is evaluated in some practical examples including other sources for stress concentration.

4.1. Rectangular plate with concentrated load

Rectangular plate $6\times2\times0.01\,m^3$ with a longitudinal concentrated force $0.01\,N$ made from a material with $E=207\,GPa$ and $\nu=0.3$ is considered, as representative of the problem with stress concentration due to concentrated force. Figure 10 demonstrates the geometry and loading condition of the whole model, initial coarse mesh generated for a quarter of the whole symmetric model and the selected paths around the model.

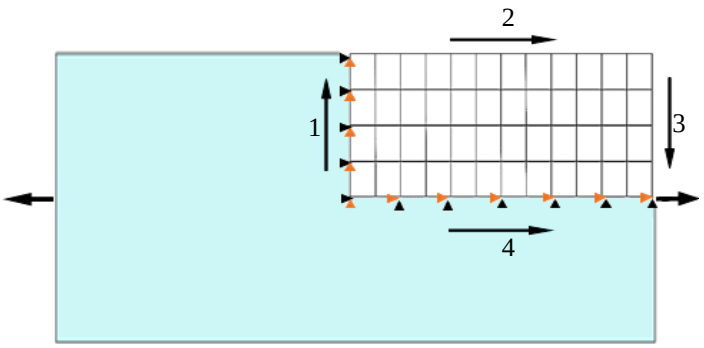

Fig. 10. The geometry, load, initial coarse mesh and paths for the model

The Mesh refinement process is conducted based on the developed algorithm. Figure 11 shows the trend of convergence along the path 4. As it shows, the convergence has reached properly after only 4 mesh refining processes except for the end part of the path 4 which is closed to the loading point. From the elasticity equations governing the problems with concentrated load (Flamant problem), the loading point is a single point having infinite stress value [19]. Therefore, the refining process stopped based on the convergence in other paths. Figure 12 shows this convergence along the path 2. Figure 13 shows generated mesh after the noted number of the refining process.

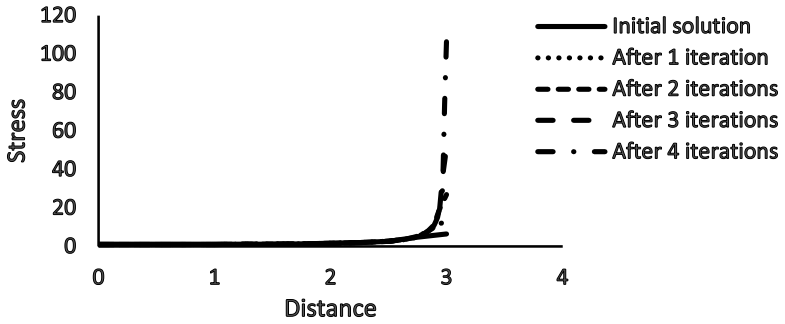

Fig. 11. Convergence trend along the path 4

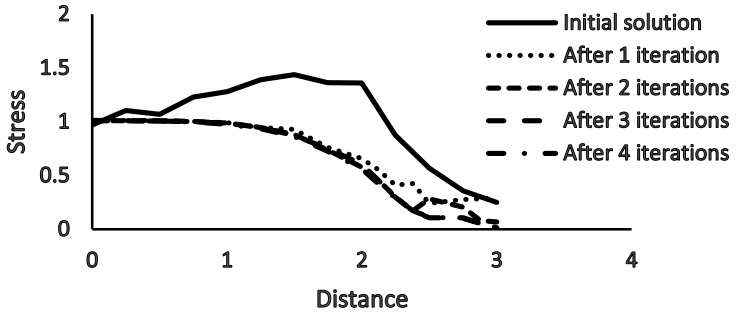

Fig. 12. Convergence trend along the path 2

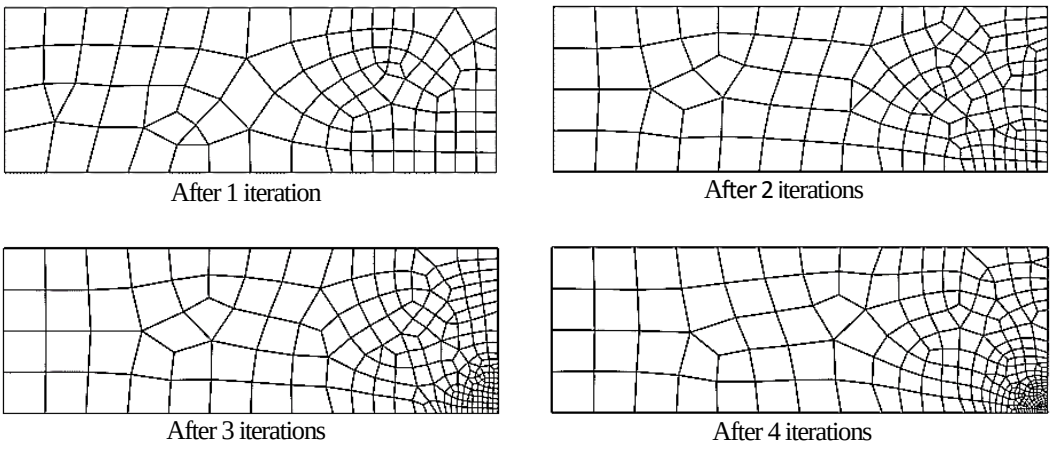

Fig. 13. Generated meshes after the noted number of the refining process

Figure13 demonstrates that the algorithm works properly; since the mesh is significantly fine closed to loading region. Figure 14 shows the proposed optimum mesh for the whole model.

4.2. Rectangular bimaterial plate with distributed load

Square plate $4\times4\times0.01\,m^3$ with a square hole $1.5\times1.5\times0.01\,m^3$ at the center is loaded with $1\,MPa$ distributed pressure in all four sides, the internal square hole is filled with a material with $E_{in}=0.01GPa$ and $\nu_{in}=0.49$, while the surrounding square is made of a material with $E_{out}=207\,GPa$, $\nu_{out}=0.3$. This example represents stress concentration due to sudden change in material. Figure 15 demonstrates the geometry and loading condition of the whole model, initial coarse mesh generated for a quarter of the whole symmetric model and the selected paths around the model. The mesh refinement process is conducted based on the developed algorithm. Figure 16 shows the trend of convergence along the path 2. Figure 17 shows generated mesh after the noted number of the refining process.

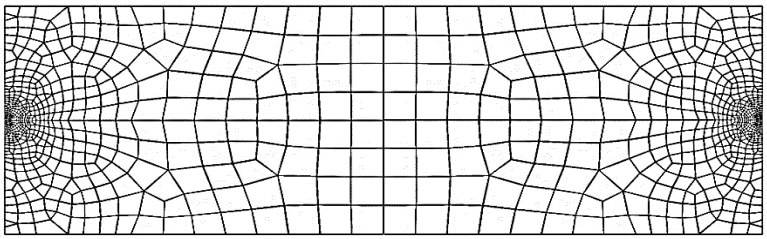

Fig. 14. Optimum mesh obtained by presented algorithm

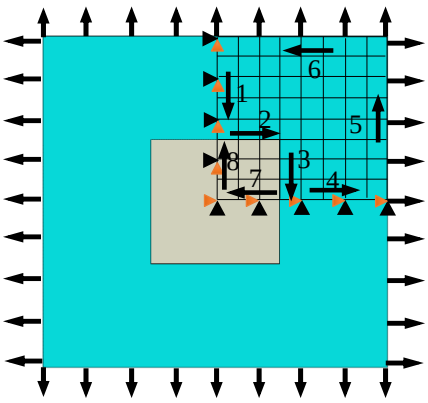

Fig. 15. The geometry, load, initial coarse mesh and paths for the model

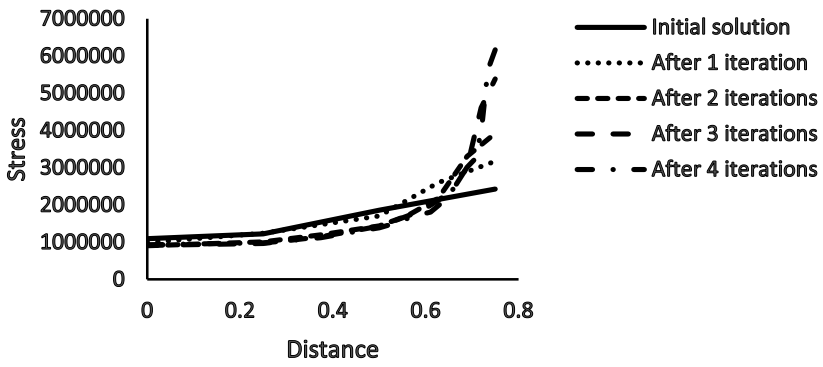

Fig. 16. Trend of convergence along the path 2

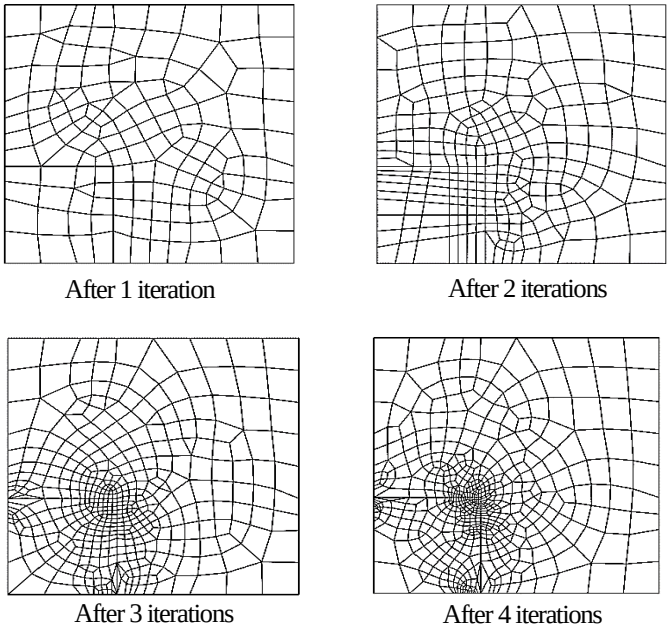

Fig. 17. Generated meshes after the noted number of the refining process

As it can be seen in Figure 16 the solution converges properly; since the fine mesh is generated around the region corresponding to sudden material changes (Fig. 17). Figure 18 shows the optimum mesh for the whole model.

4.3. Mesh generation of fiber reinforced polymer materials

Gonzalez and Lorca [3] studied the mechanical behavior of fiber reinforced polymer materials. They built the FE model implementing uniform mesh. To obtain convergence for the solution, they used extremely fine mesh. This example includes a combination of several stress concentration sources including concentrated force and sudden changes in geometry and material. As a more general problem, an arbitrary part of the whole geometry is considered which includes a complete circular section of one fiber as well as small parts of two other fibers.

The model is built based on the same material property in plane strain condition with 6-node quadratic is oparametric triangle elements (CPE6M) [1]. Figure 19 demonstrates the geometry and loading condition of the model, initial coarse mesh, and the selected paths around the model. The mesh refinement process is conducted based on the developed algorithm. Figure 20 shows the trend of convergence along the path 3.

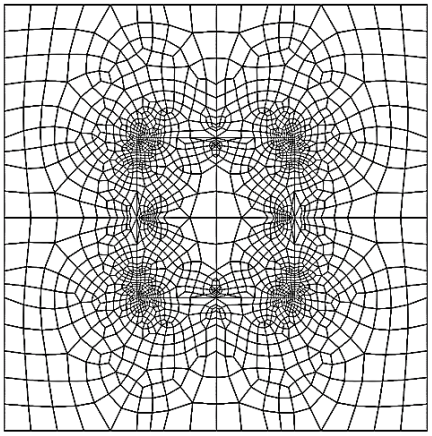

Fig. 18. Optimum mesh obtained by presented algorithm

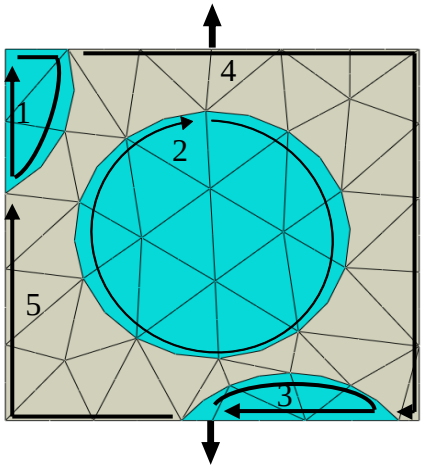

Fig. 19. The geometry, load, initial coarse mesh and paths for the model

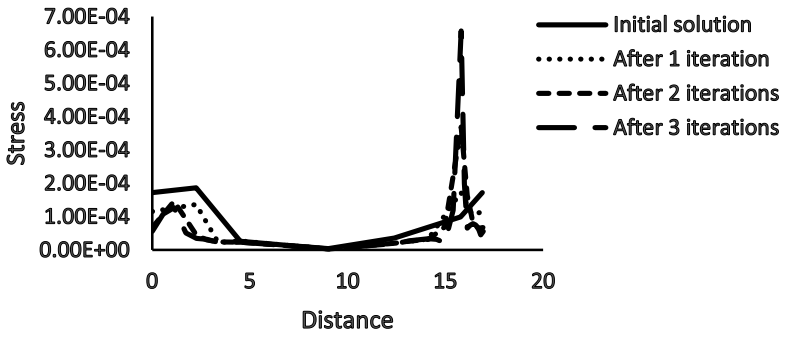

Fig. 20. Trend of convergence along the path 3

As it shows ,in Figure 20 the solution convergence is only after 3 refining steps except at the load exertion point. Similar discussion as mentioned in Figure 11 can be noted again here.

To investigate the convergence, the other paths are considered. Figures 21 to 24 demonstrate proper convergence of stress curves along paths 1, 2, 4 and 5, respectively. Figure 25 shows generated mesh after the identified number of the refining process.

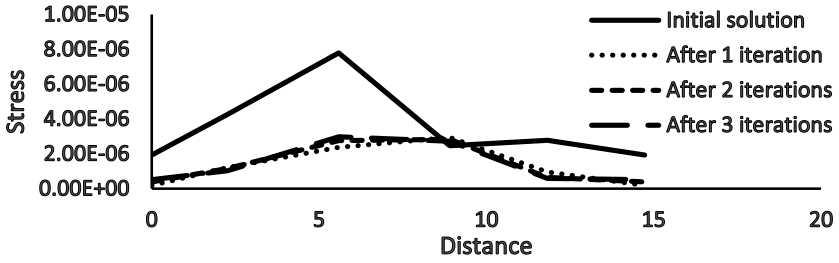

Fig. 21. Trend of convergence along the path 1

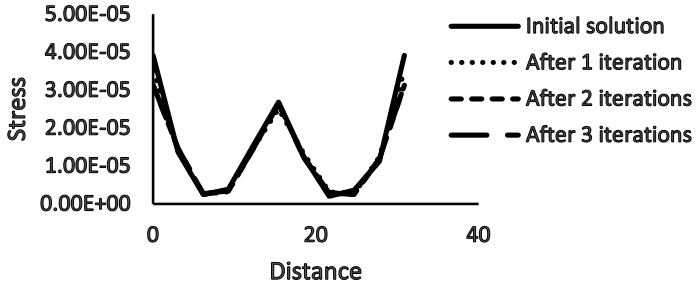

Fig. 22. Trend of convergence along the path 2

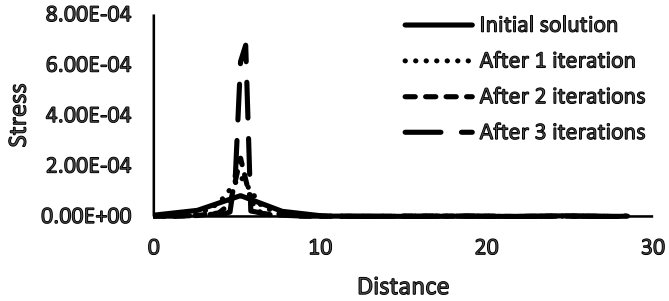

Fig. 23. Trend of convergence along the path 4

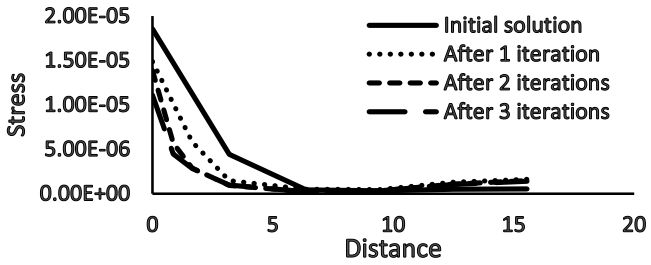

Fig. 24. Trend of convergence along the path 5

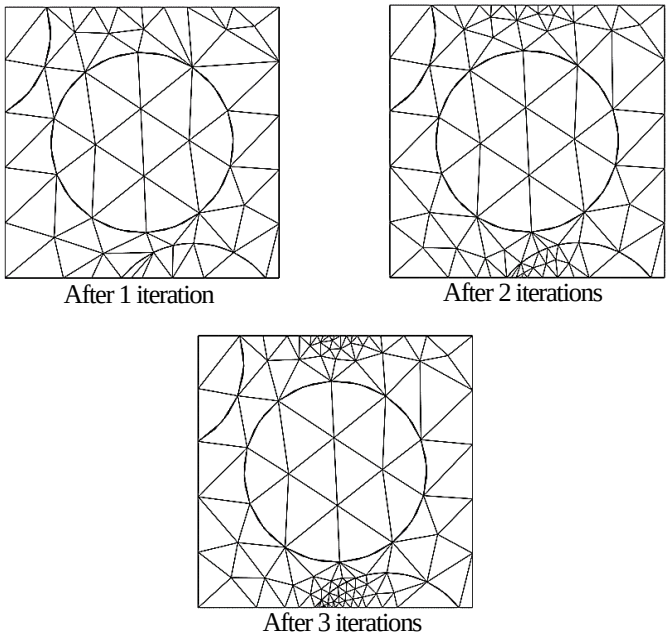

Fig. 25. Generated meshes after the noted numbers of the refining process

In this example, there exist all three types of stress concentration sources; while Figure 25 shows distinguishably finer mesh in the region of force exerted. As mentioned before, this is a single point with infinite stress value. Because of extremely rapid change in the stress in this point, the element only in this region is recognized as the main improper elements in each step of refining procedure.

Since the convergence is obtained suitably, the mesh refined at the third refining step is proposed as optimum mesh which is compared with the mesh used by Gonzalez and Lorca [3] in Figure 26.

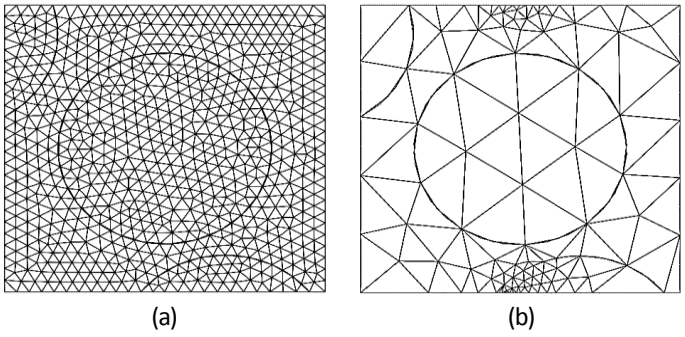

Fig. 26. (a) Uniform mesh used by Gonzalez and Lorca [3]; (b) optimum mesh identified by the algorithm

Figures 27 and 28 compare the variation of stress along paths 2 and 4 obtained using two meshes shown in Figure 26.

In Figures 27 and 28 good agreement can be observed seen between the results obtained using two meshes, except at the load point; Therefore, the developed algorithm presents mesh with less number of elements as well as more desired distribution.

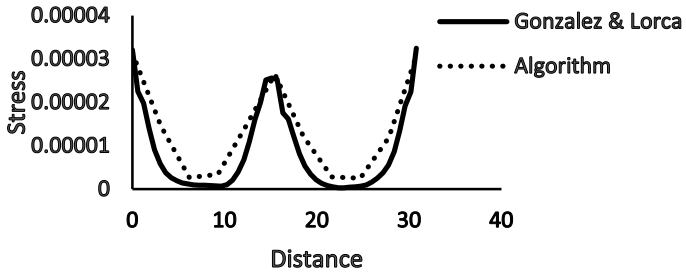

Fig. 27. Stress along path 2

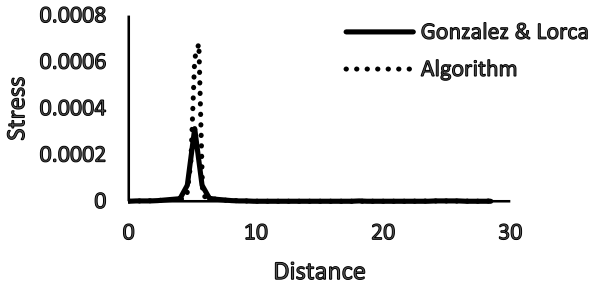

Fig. 28. Stress along path 4

5. Conclusions

This adaptive mesh generation procedure is able to distribute element with different size of element in the analysis domain properly. This is a great modification compared to convergence procedure required for uniform mesh generation. In addition, it usually converges after a few refinement steps. The average of elemental stress derivatives is indicated as suitable limit value for the element refining process. Implementing this algorithm the convergence is fast and accurate enough compared to options available in Abaqus. Several examples studied in this study demonstrate that the described mesh generator senses all sources for sudden changes in output parameters successfully. Therefore, it proposes the optimum mesh to capture the behavior of bimaterials specifically at interfaces. This procedure has the potential to be computerized as a subroutine for commercial FE software in order to automatically generate optimum mesh after some preliminary solutions.

References

[1]. Abaqus, User's Manual, Dassault Systèmes Simulia Corp, 2012.

[2]. Ansys, Tutorial Release 14.5, SAS IP, Inc., 2012.

[3]. C. Gonza´lez and J. LLorca, "Mechanical behavior of unidirectional fiber-reinforced polymers under transverse compression: Microscopic mechanisms and modeling," *Composites Science and Technology*, vol. 67, p. 2795–2806, 2007.

[4]. Laurent Van Miegroet, Pierre Duysinx, Stress concentration minimization of 2D filets using X-FEM and level set description, Struct Multidisc Optim (2007) 33:425–438.

[5]. C. Lee and R. Hobbs, "Automatic adaptive ®nite element mesh generation over arbitrary two-dimensional domain using advancing front technique," *Computers and Structures*, no. 71, pp. 9-34, 1999.

[6]. R. Montenegro, J. Cascón, J. Escobar, E. Rodríguez and G. Montero, "An automatic strategy for adaptive tetrahedral mesh generation," *Applied Numerical Mathematics*, no. 59, p. 2203–2217, 2009.

[7]. S. Phongthanapanich, "Delaunay Adaptive Remeshing Technique for Finite Element/Finite Volume Methods," Thailand, 2010.

[8]. S. Lo, "Dynamic grid for mesh generation by the advancing front method," *Computers and Structures*, no. 123, p. 15–27, 2013.

[9]. G. H. Paulino, I. F. M. Menezes, J. B. Cavalcante Neto, L. F. Martha, A methodology for adaptive finite element analysis: Towards an integrated computational environment, Computational Mechanics 23 (1999) 361-388.

[10]. K.S.R.K. Murthy and M. Mukhopadhyay, Adaptive finite element analysis of mixed-mode fracture problems containing multiple crack-tips with an automatic mesh generator, *International Journal of Fracture* 108: 251–274, 2001.

[11]. Guoqun Zhao, Hongmei Zhang, Lianjun Cheng, Geometry-adaptive generation algorithm and boundary match method for initial hexahedral element mesh, Engineering with Computers (2008) 24:321–339

[12]. Xinghua Liang , Yongjie Zhang, An octree-based dual contouring method for triangular and tetrahedral mesh generation with guaranteed angle range, Engineering with Computers (2014) 30:211–222

[13]. Lu Sun, Guoqun Zhao, Adaptive hexahedral mesh generation and quality optimization for solid models with thin features using a grid-based method, Engineering with Computers, DOI 10.1007/s00366-015-0399-9, Published online, 14 Feb 2015.

[14]. Alshoaibi, Abdulnaser M., Ariffin, Ahmad Kamal, Finite element simulation of stress intensity factors in elastic-plastic crack growth, Journal of Zhejiang University SCIENCE A, *2006 7(8):1336-1342*.

[15]. E. Ruiz-Girones, X. Roca, J. Sarrate, Size-preserving size functions and smoothing procedures for adaptive quadrilateral mesh generation, Engineering with Computers (2015) 31:483–498

[16]. A. Rajagopal, S. M. Sivakumar, A combined *r-h* adaptive strategy based on material forces and error assessment for plane problems and bimaterial interfaces, Comput Mech (2007) 41:49–72.

[17]. James P. Carson, Andrew P. Kuprat, Xiangmin Jiao, Volodymyr Dyedov, Facundo del Pin, Julius M. Guccione, Mark B. Ratcliffe, Daniel R. Einstein, Adaptive generation of multimaterial grids from imaging data for biomedical Lagrangian fluid–structure simulations, Biomech Model Mechanobiol (2010) 9:187–201.

[18]. C. Li, C. Song, H. Man, E.T. Ooi, W. Gao, " HYPERLINK "http://www.sciencedirect.com/science/article/pii/S0020768314000626" 2D dynamic analysis of cracks and interface cracks in piezoelectric composites using the SBFEM ," *International Journal of Solids and Structures*, vol. 51, no. 11–12, P. 2096-2108, 2014.

[19]. M. H. Sadd, Elasticity: Theory, Applications, and Numerics, Burlington: Elsevier Inc, 2005.

[20]. J. D. Hoffman, Numerical methods for engineers and scientists, 2nd edition, New York: Marcel Dekker, Inc., 2001.